Journal of Exercise Physiologyonline

August 2013
Volume 16 Number 4

JEPonline

Official Research Journal of the American Society of Exercise Physiologists

ISSN 1097-9751

FoxO1 Inhibits Skeletal Muscle Hypertrophy Through mTOR-independent Mechanisms

Rachael A. Potter[1], Alissa D. DeLong[1], Sierra M. Smith[1], Benjamin M. Erb[1], Bryon Renwand[1], Yasutomi Kamei[2], Yoshihiro Ogawa[2], and Thomas J. McLoughlin[1]

[1]Department of Kinesiology, The University of Toledo, Toledo, Ohio, [2]Medical Research Institute, Tokyo Medical and Dental University, Tokyo

ABSTRACT

Potter RA, DeLong AD, Smith SM, Erb BM, Renwand B, Kamei Y, Ogawa Y, McLoughlin TJ. FoxO1 Inhibits Skeletal Muscle Hypertrophy Through mTOR-independent Mechanisms. **JEPonline** 2013;16(4):32-50. The canonical Akt/mTOR signaling pathway plays a strong role in promoting skeletal muscle hypertrophy through regulating anabolic and catabolic signaling cascades. The transcription factor, FoxO1, a downstream molecular target of Akt signaling, may play a negative role in skeletal muscle hypertrophy through suppression of growth signaling and/or upregulation of atrophy gene expression. Using a transgenic mouse model in which FoxO1 is specifically expressed within skeletal muscle, we tested the hypotheses: (a) that FoxO1 inhibits skeletal muscle hypertrophy in vivo; and (b) that inhibition of skeletal muscle hypertrophy conferred through FoxO1 expression is associated with suppression of Akt/mTOR signaling and upregulation of muscle atrophy F-box (MAFbx/atrogin-1) gene expression. The findings confirm that FoxO1 inhibits skeletal muscle hypertrophy associated with 2 wks of mechanical overload (synergist ablation), evidenced through dampened increases in muscle mass, protein content, and muscle cross sectional area. We conclude that FoxO1 overexpression hampers the ability of skeletal muscle to hypertrophy, and that this suppression involves mechanisms independent of mTOR signaling.

Key Words: Synergist Ablation, Ubiquitin, Anabolism, Atrophy, $p70^{s6k}$

INTRODUCTION

The regulation of skeletal muscle hypertrophy is contingent upon the fine balance between protein synthesis and degradation. Although this fine balance is maintained by a myriad of molecular signaling mechanisms, a wealth of data has implicated the canonical Akt/mTOR signal transduction pathway and associated downstream molecules (e.g., $p70^{s6k}$, 4EBP-1) as potent regulators of skeletal muscle size (5,18,24). Activation of Akt and subsequent activation of downstream molecules (e.g., mTOR) appears to play a role in promoting skeletal muscle hypertrophy through not only induction of protein synthesis machinery, but also the downregulation of protein degradation cascades. Specifically, activation of molecules within the canonical Akt/mTOR pathway appears to suppress gene expression of key muscle degradatory genes, namely the muscle atrophy F-box protein (MAFbx/atrogin-1), an E3 ubiquitin ligase that plays a critical role in regulating protein ubiquination and breakdown in skeletal muscle (4,11,30).

The ability of the Akt-mediated signaling to dictate changes in muscle size appears to be due, in part, through its influence on the transcription factor FoxO1. Specifically, FoxO1, a known target of Akt kinase activity (28), is phosphorylated and subsequently sequestered in the cytoplasm and kept removed from its nuclear target genes upon Akt activation (6,28,35). When Akt signaling is markedly suppressed, as in cases of muscle atrophy (5,8), FoxO1 accumulates in the nucleus and can promote the expression of MAFbx/atrogin-1 (16). Conversly, in cases of muscle hypertrophy, when Akt signling is activated, FoxO1 has been shown to be hyperphosphorylated and sequestered in the cytoplasm (19).

Using an in vivo muscle specific overexpression model, Kamei et al. (16) reported that mice that overexpress FoxO1 had decreased muscle size, which was accompanied by increased gene expression of known muscle atrophy-associated genes (e.g., MAFbx/atrogin-1, lysosomal proteinase, capthesin-L). Given that activation of FoxO1 has been shown to promote the specific degradation of key anabolic signaling molecules, specifically mTOR and $p70^{s6k}$ (34), it is resonable to speculate that amplification of FoxO1 activity has a negative impact on muscle size, in part through hampering growth signaling. Although yet to be explored, given its potent role in the regulation of muscle hypertrophy (3,5), FoxO1 may act to hinder skeletal muscle hypertrophy upon exposure to growth stimulus (e.g., mechanical overload) through disruption of Akt and mTOR mediated growth signaling.

The purpose of this investigation was to test the hypotheses: (a) that FoxO1 overexpression in skeletal muscle suppresses hypertrophy; and (b) that the suppression is associated with compromised Akt, mTOR, $p70^{s6k}$, and 4EBP-1 signaling (i.e., phosphorylation status) and increased MAFbx/atrogin-1 gene and protein expression. These hypotheses were tested using a transgenic mouse model in which the FoxO1 protein is specifically overexpressed within skeletal muscle (16). Muscle hypertrophy was induced via a synergist ablation surgical model, in which the plantaris muscle was chronically overloaded for a period of 2 wks (12).

METHODS

Subjects

Animals: Three-month-old male wildtype C57BL/6 (WT) and skeletal muscle specific FoxO1 overexpressing mice ($FoxO1^{+/-}$, C57BL/6 background) used in the experiments were obtained from an established breeding colony at The University of Toledo. FoxO1 overexpression was driven within skeletal muscle of transgenic mice via a skeletal muscle actin promoter, as previously described (16). All procedures were performed in accordance with University of Toledo Institutional Animal Care and

Use Committee guidelines. All animals were housed in clear polycarbonate cages, exposed to a 12:12 hr light-dark cycle (lights on at 0800 hrs), and provided a standard rodent diet and water ad libitum. For all experiments, Line A2 FoxO1$^{+/-}$ mice were used, as these mice possess the highest FoxO1 transgene copy number incorporation and, therefore, express the highest amount of the FoxO1 protein (16).

Animal Surgeries: Following genotypic determination, FoxO1$^{+/-}$ and WT mice were divided into two groups (n = 10-12 per group): (a) 14-day sham surgery (control); and (b) 14-day synergist ablation (overload). All mice were anesthetized with an intraperotineal injection of 2.5% Avertin. Following anesthetization, a small incision over the posterolateral aspect of the lower hindlimb was made, exposing the plantaris, soleus, and gastrocnemius muscles, as previously described (12). The synergist soleus and gastrocnemius muscles were excised, leaving the plantaris muscle intact (synergist ablation overload model). This was performed bilaterally on all animals. Animals exposed to a sham surgery (animals anesthetized, muscle exposed and the incision sutured without removing the muscles) served as controls. The incisions were then closed and animals returned to their cages and allowed to resume normal cage activity. Non-surgery control mice initially included in the study were found to be not statistically different from sham-control mice on any of the dependent variables measured. As such, non-surgery controls were subsequently pooled with sham-controls for all analyses (data not shown).

Procedures

Muscle Collection and Protein Quantification: Following 14-days of normal cage activity, control mice and mice exposed to synergist ablation (mechanical overload) were anesthetized and plantaris muscles excised, cleaned of any residual connective tissue, weighed, snap frozen in liquid nitrogen and stored at −80ºC for subsequent analysis. Plantaris muscles were homogenized in PKB buffer supplemented with HALT™ protease inhibitor single-use cocktail (Thermo Scientific, Rockford, IL) and 10 mM Na_3VO_4 using a TissueLyser (2 x 3.0 min at 30 Hz; Qiagen, Valencia, CA). Homogenates were spun at 14,000 x *g* for 15 min at 4^{o}C and the supernatants were removed and rapidly frozen at −80ºC. Protein concentrations of the supernatants were subsequently determined using detergent-compatible protein assay kit (DC Protein Assay, Bio-Rad, Hercules, CA) and quantified by spectrophotometry using a microtiter plate reader (SpectraMax 190; Molecular Devices, Sunnyvale, CA). For determination of FoxO1 protein content and cellular localization, cytoplasmic and nuclear fractions were obtained via use of a commercially available extraction kit (ProteoJET; Fermentas Life Sciences, Glen Burnie, MD).

Histology: Control and overloaded plantaris muscles from a separate cohort of mice were excised, mounted in tissue freezing medium, and frozen in liquid nitrogen pre-cooled isopentane. Serial muscle sections (10 μm) were stained with hematoxylin and eosin and sections visualized using an Olympus IX70 fluorescence microscope (Melville, NY) equipped with a digital camera and image processing software (Spot-RT, Diagnostic Instruments, Inc., Sterling Heights, MI). Muscle fiber CSA of all muscle fibers in each of the collected control and mechanically overloaded sections were digitized and quantified using Image-PRO Plus software (Media Cybernetics, Bethesda, MD) by a blinded experimenter. When the automated approach failed and there was not 100% fidelity, the expermineter manually verified that all muscle fiber borders had been traced.

Western Blotting: Muscle homogenates (50 μg) were solubilized in Laemmeli sample buffer and boiled for 5 min, resolved by SDS-PAGE on 6% (mTOR),7.5% (FoxO1, p70^{s6k}, and Akt), 10% (MAFbx/atrogin-1) or 16% (4EBP-1) tricine or polyacrylamide gels, transferred to a polyvinyl difluoride membrane (PVDF-FL; Millipore; Billerica, MA) via either wet-transfer (mTOR; Hoefer TE-22; 400mA constant for 2 hrs; 4EBP-1; Hoefer TE-22; 200mA constant for 1 hr) or semi-dry blotting (FoxO1, Akt,

$p70^{s6k}$, and MAFbx/atrogin-1; TransBlot Transfer Cell, Bio-Rad Laboratories, Inc., Hercules, CA; 20v constant for 1 hr), blocked in 5% non-fat dry milk in TBS for 1 hr at room temperature, and immunoblotted overnight at 4ºC with total-mTOR, phospho-mTOR (Ser^{2448}), total FoxO1, total-$p70^{s6k}$, phospho-$p70^{s6k}$ (Thr^{389}), total Akt, and phospho-Akt (Ser^{473}), total 4EBP-1, phospho-4EBP-1 ($Thr^{37/46}$) and MAFbx/atrogin-1 antibodies (1:1000; Cell Signaling, Beverley, MA). Equal protein loading was verified using GAPDH expression (1:5000; Cell Signaling, Beverley, MA). After a 1 hr incubation with an infrared-conjugated Alexa Fluor 680 secondary antibody (1:5000; Molecular Probes, Carlsbad, CA) at room temperature, the immunoreactive proteins were observed via infrared detection (Odyssey Imaging System, LI-COR BioSciences, Lincoln, NE) and quantified by densitometry.

Immunoprecipitation: Muscles samples were homogenized in NP-40 buffer (50mM Tris base, 150 mM NaCl, 1% NP-40, pH 8.0) containing HALT™ protease inhibitor single-use cocktail supplemented with 10 mM Na_3VO_4 and spun at 14,000 x g for 15 min at 4°C; supernatants were collected and used for immunoprecipitation reactions. Supernatants were pre-cleared using a slurry of protein A/G magnetic beads (Invitrogen, Carlsbad, CA) for 1 hr at 4º C and then incubated overnight at 4ºC with a total mTOR antibody (1:100; Cell Signaling). Following the overnight incubation, muscle/antibody complexes were incubated for 1 hr with a slurry of protein A/G magnetic beads at 4ºC. The magnetic beads were then isolated using a DynaMag magnet (Invitrogen), washed with NP-40 buffer, solubilized in Laemmeli sample buffer, and heated to 95ºC in preparation for SDS-PAGE. Following SDS-PAGE, western blotting was performed using antibodies against phosphorylated and total mTOR (1:1000). Following 1 hr incubation with an infrared-conjugated Alexa Fluor 680 secondary antibody (1:5000) at room temperature, the immunoreactive proteins were observed via infrared detection (Odyssey Imaging System, LI-COR BioSciences, Lincoln, NE) and quantified by densitometry.

Real-time Quantitative PCR (qRT-PCR): Total RNA was isolated from control and overloaded WT and $FoxO1^{+/-}$ plantaris muscles using an RNeasy Mini column (Qiagen, Valencia, CA), purified by DNase digestion (Turbo DNase; Ambion, Foster City, CA), and stored at −80°C until further processing. cDNA synthesis using 10 ng of total RNA and subsequent PCR amplification was performed using a one-step qRT-PCR kit (Superscript III, Invitrogen) and gene specific Taqman® primers and probes (Applied Biosystems, Foster City, CA) designed against MAFbx (Mm00499518_m1) and GAPDH (Mm99999915_g1). The qRT-PCR reactions were carried out in triplicate using a Applied Biosystems7500 Real-Time Detection System. Analyses were performed to verify the dynamic range and confirm consistency among the amplification efficiencies of the various target genes analyzed. Data were expressed via the comparative C_t method, in which ΔCt values were calculated for all samples as follows: $Ct_{target\ gene} - Ct_{housekeeping\ gene}$, where the target gene was MAFbx and the housekeeping gene was GAPDH. Relative changes in gene expression were then calculated for each target gene via the $2^{-\Delta\Delta Ct}$ method, in which ΔCT values determined for each of the experimental samples (WT ablation, $FoxO1^{+/-}$ control and $FoxO1^{+/-}$ ablation) were subtracted from the ΔCT value from the calibrator sample (WT control).

Ubiquination Assays: Muscle homogenates from control and overloaded WT and $FoxO1^{+/-}$ mice were subjected to immunoprecipitation via magnetic bead separation, as described previously. Briefly, pre-cleared homogenates were incubated overnight with ubiquitin antibody (1:100; SC-8017, Santa Cruz Biotechnology Inc., Santa Cruz, CA). Immunoprecipitated proteins were resolved by SDS-PAGE on 4-15% polyacrylamide gradient gels (Jule Inc., Milford, CT). After which, gels were incubated overnight in Krypton Protein Stain (21)(Thermo Scientific, Rockford, IL) and then observed via infrared detection (Odyssey Imaging System, LI-COR BioSciences, Lincoln, NE), as previously described (21).

Statistical Analyses

Differences in FoxO1 protein expression between wildtype and FoxO1$^{+/-}$ mice were analyzed via independent student *t*-test. Cytoplasmic and nuclear localization of total FoxO1 protein were analyzed using a three-way factorial ANOVA (strain [wildtype vs. FoxO1$^{+/-}$] x treatment [control vs. ablation] x fraction [cytoplasmic vs. nuclear]. Where a significant effect was found, multiple comparison analysis was performed with the Sidak post hoc test to identify differences. All subsequent data obtained were analyzed with a two-way factorial ANOVA (strain [wildtype vs. FoxO1$^{+/-}$] x treatment [control vs. ablation]) with a Student-Newman-Keuls post hoc analysis used to locate difference when a significant interaction effect was found. The alpha level was set at $P<0.05$ a priori and was used for determination of statistical significance in all statistical procedures.

RESULTS

FoxO1 expression inhibits skeletal muscle hypertrophy. As shown in Figure 1, plantaris muscles of FoxO1$^{+/-}$ mice displayed significant elevations in FoxO1 total protein expression compared to WT counterparts.

Figure 1

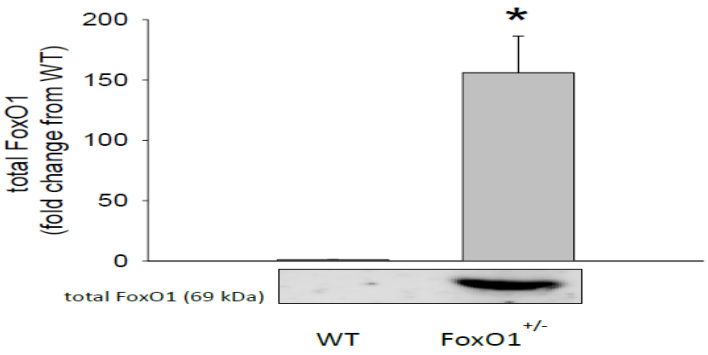

Figure 1. Total FoxO1 Protein Expression is Elevated in Plantaris Muscles of FoxO1$^{+/-}$ Mice Compared to Wildtype (WT) Mice. Panel A: Total FoxO1 protein in WT and FoxO1$^{+/-}$ mice. *, significant difference between FoxO1$^{+/-}$ and WT mice. $P<0.05$ for all significant differences. n = 6 for each group. Data represented as means ± standard error.

Body masses of FoxO1$^{+/-}$ mice were significantly smaller than that of age-matched WT mice, as previously reported by Kamei et al. (16). No significant difference in body mass was observed between control and overload conditions for WT and FoxO1$^{+/-}$ mice. When the data were normalized to body mass, no differences in control plantaris muscle mass or protein content were observed between WT and FoxO1$^{+/-}$ mic. The plantaris muscles of WT mice and FoxO1$^{+/-}$ mice exhibited a significant increase in both relative (60% and 27%, respectively) and absolute (58% and 25%, respectively, data not shown) mass following overload (Table 1). This finding was corroborated by

significant increases in relative (61% and 12%, respectively) and absolute (51% and 19%, data not shown) protein contents.

Table 1. Body mass, normalized muscle mass and normalized protein content for wildtype and FoxO1 transgenic control or mechanically overloaded mice.

Condition	*Treatment*	*Body Mass (g)*	*mg muscle/ g body mass*	*% Change from Control (relative mass)*	*mg protein/ g body mass*	*% Change from Control (relative protein)*
Wildtype	Control	$25.2 \pm 0.45^{\&}$	0.68 ± 0.02	–	0.054 ± 0.006	–
	Overloaded	26.2 ± 0.47	$1.09 \pm 0.02^{*\#}$	↑ 60%	$0.087 \pm 0.006^{*\#}$	↑ 61%
FoxO1	Control	20.7 ± 0.47	0.66 ± 0.02	–	0.055 ± 0.006	–
	Overloaded	20.2 ± 0.45	$0.84 \pm 0.02^{*}$	↑ 27%	$0.062 \pm 0.005^{*}$	↑ 12%

&= sig. main effect for condition (wildtype sig. greater than FoxO1), *= sig diff. from control, #= sig diff. from control and ablation for both WT and FoxO1. $p < 0.05$ for all comparisons. n=8-10 muscles per group.

Although both mouse strains exhibited increases in muscle mass and soluble protein content following the mechanical overload compared to their respective controls, the changes observed in the FoxO1$^{+/-}$ mice were significantly muted compared to WT counterparts. In control muscle, fiber cross-sectional area of WT mice was significantly greater than that of FoxO1$^{+/-}$ mice (Figure 2A), with the majority of the muscle fibers in FoxO1$^{+/-}$ plantaris muscles being <500 μm^2 (Figure 2B). Muscle cross-sectional area of WT mice increased upon exposure to mechanical overload compared to control and was significantly greater than that of FoxO1$^{+/-}$ mice. The hypertrophic response was significantly blunted in FoxO1$^{+/-}$ mice compared to WT mice 4.5% vs. 32% hypertrophy, respectively; Figure 2C) and was not statistically significant from control. No significant differences were observed in the number of muscle fibers between WT and FoxO1$^{+/-}$ (control muscle; 582 ± 31.8 vs. 525 ± 50, respectively; data not shown).

Figure 2

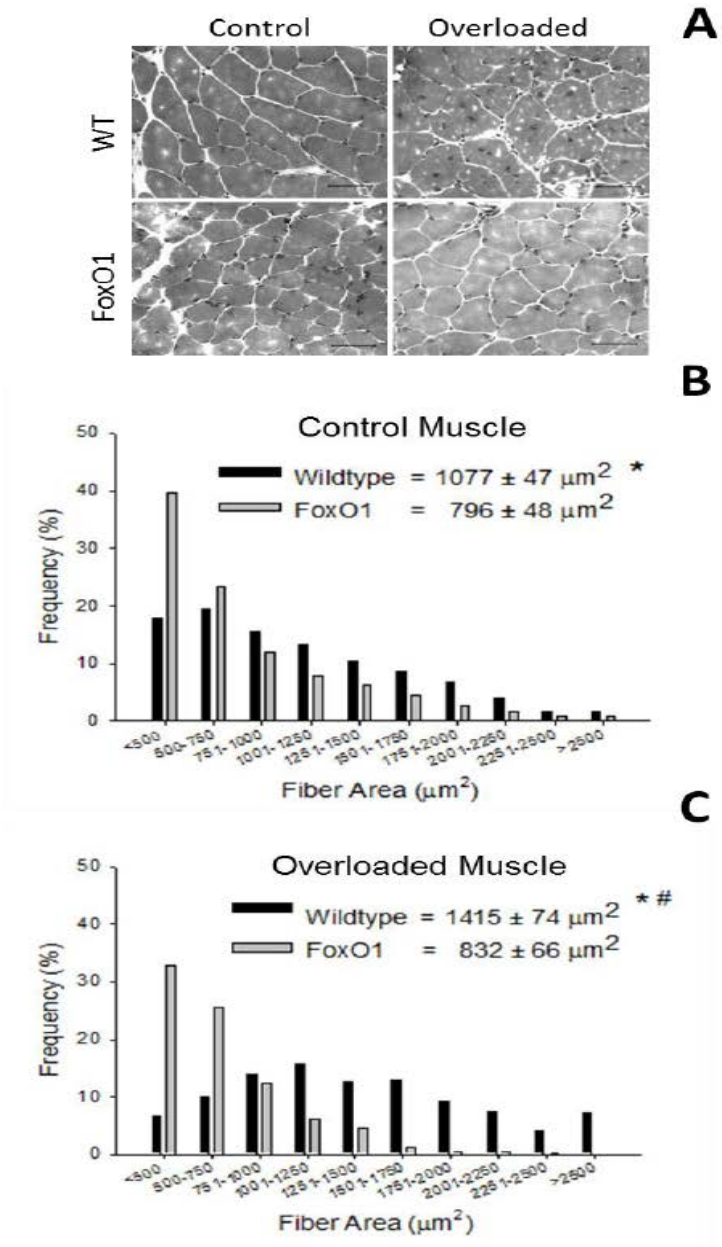

Figure 2. Plantaris Muscle Cross-Sectional Area is Smaller and Does Not Significantly Increase Following Overload in FoxO1$^{+/-}$ Mice. Panel A: Hematoxylin and eosin staining of control and overloaded (ablation) plantaris muscles of wildtype (WT) and FoxO1$^{+/-}$ mice. Panel B: Frequency histogram of muscle cross-sectional areas of control plantaris muscles of WT and FoxO1$^{+/-}$ mice. &, significant main for effect strain; #, significant difference between WT and FoxO1$^{+/-}$ mice in control plantaris muscle. Panel C: Frequency histogram of muscle fiber cross-sectional areas of overloaded plantaris muscles of WT and FoxO1$^{+/-}$ mice. %, significant main effect for treatment; *, significant difference from respective control. #, significant difference between WT and FoxO1$^{+/-}$ mice in overloaded plantaris muscle. $P<0.05$ for all significant differences. n=8-10 for all groups. Data represented as means ± standard error.

FoxO1-mediated inhibition of muscle hypertrophy is not associated with suppression of mTOR and p70^{s6k} signaling. Akt phosphorylation (Ser^{473}) was significantly elevated in the muscles of FoxO1$^{+/-}$ mice compared to WT counterparts; however, mechanical overload did not differ from control as a whole (Figures 3A and 3B). Although mechanical overload resulted in elevations in total Akt in plantaris muscles of WT and FoxO1$^{+/-}$ mice compared to control (Figures 3A and 3C), the response in total Akt was similar in WT and FoxO1$^{+/-}$ mice (Figure 3C). Further, there was no significant strain by treatment interaction on protein levels of phosphorylated or total Akt.

Figure 3

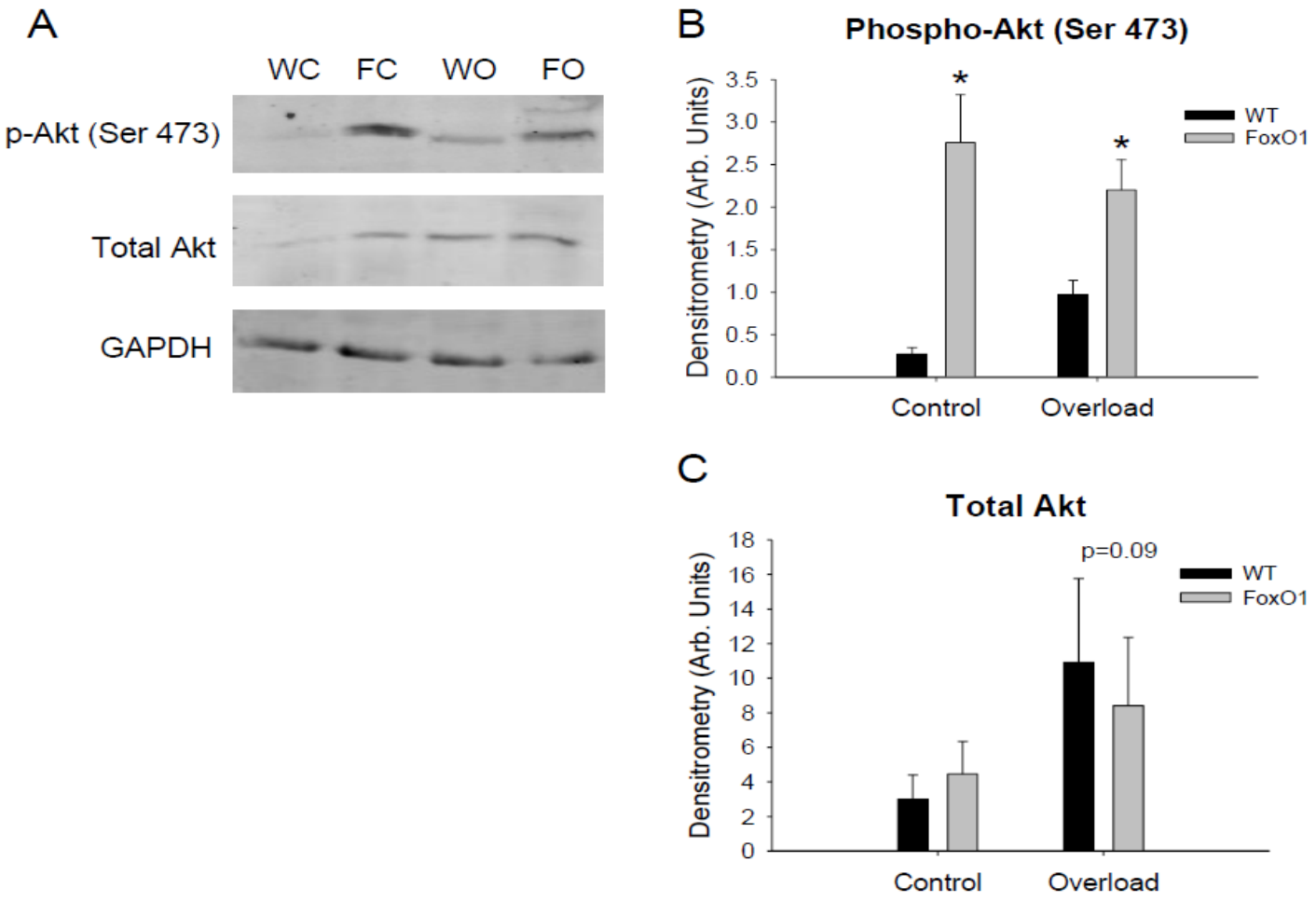

Figure 3. Phosphorylated and Total Akt Protein in Control and Overloaded Plantaris Muscles of Wildtype and FoxO1$^{+/-}$ Mice. Panel A: Representative western blot analyses from wildtype control (WC), FoxO1$^{+/-}$ control (FC), wildtype ablation (WO) and FoxO1$^{+/-}$ ablation (FO) conditions. Panels B and C: Quantification of western blot data for phosphorylated and total Akt, respectively. &, significant main effect for strain; *, trend for significant main effect treatment (P=0.09). P<0.05 for all significant differences. n=6 for all groups. Data represented as means ± standard error.

Mechanical overload resulted in a significant increase in phosphorylated mTOR (Figures 4A and 4B) and total mTOR (Figures 4A and 4C), but no significant differences between mouse strains were noted. No significant strain by treatment effect was evident in phosphorylated or total mTOR protein levels.

Figure 4

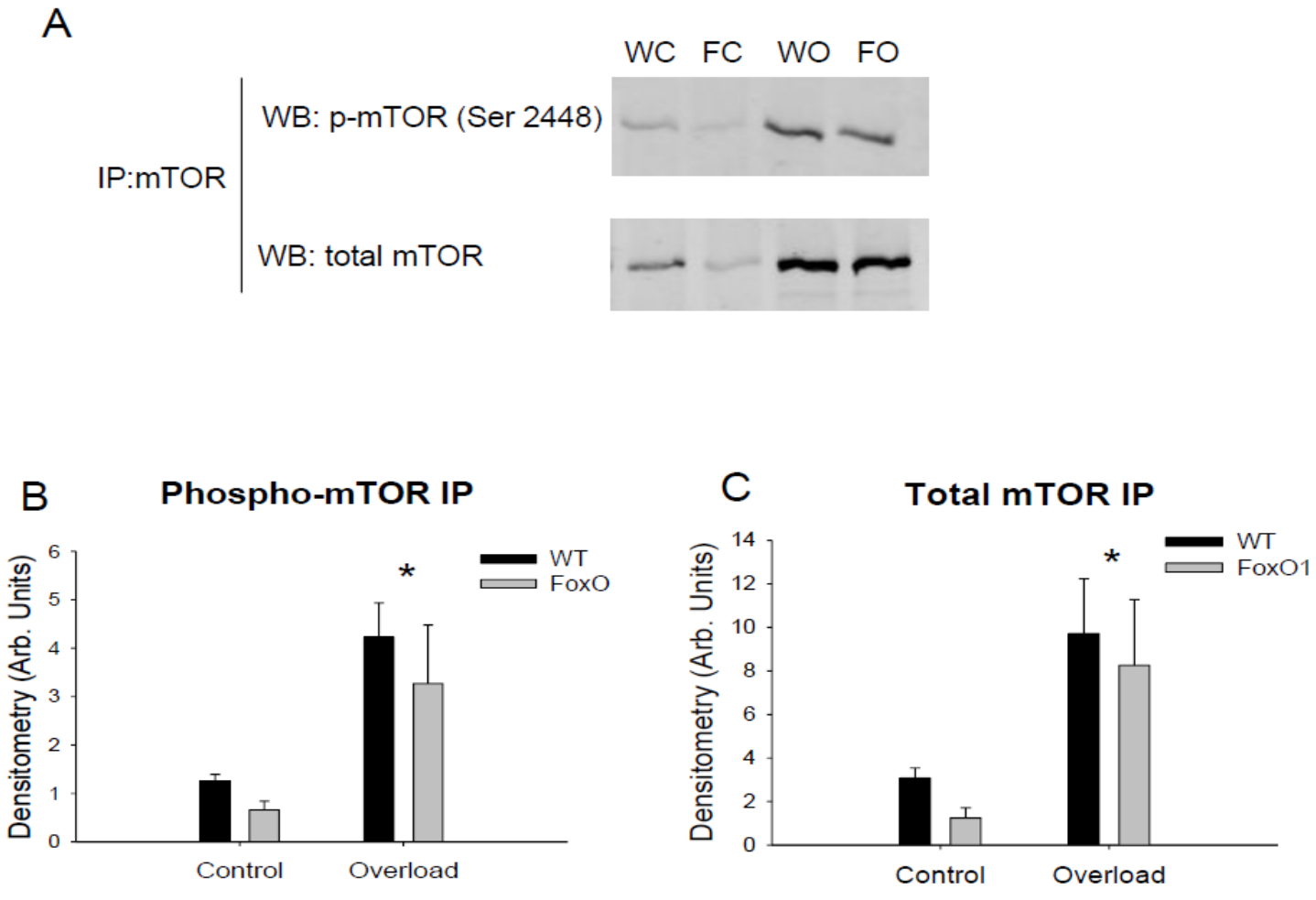

Figure 4. Immunoprecipitated Phosphorylated and Total mTOR Protein in Control and Overloaded Plantaris Muscles of Wildtype and FoxO1$^{+/-}$ Mice. Panel A: Representative western blot (WB) analyses of immunoprecipitated (IP) phosphorylated (p-mTOR) and total mTOR protein from wildtype control (WC), FoxO1$^{+/-}$ control (FC), wildtype ablation (WO) and FoxO1$^{+/-}$ ablation (FO) conditions. Panels B and C: Quantification of western blot data for phosphorylated and total mTOR, respectively. * significant main effect for treatment. $P<0.05$ for all significant differences. n=3 for all groups. Data represented as means ± standard error.

Phosphorylated (Figures 5A and 5B) and total (Figures 5A and 5C) $p70^{s6k}$ were significantly elevated in plantaris muscles following mechanical overload compared to control muscle though no overall differences between WT and $FoxO1^{+/-}$ mice were apparent. As with the upstream proteins, no strain by treatment effect was noted in phosphorylated or total $p70^{s6k}$.

Figure 5

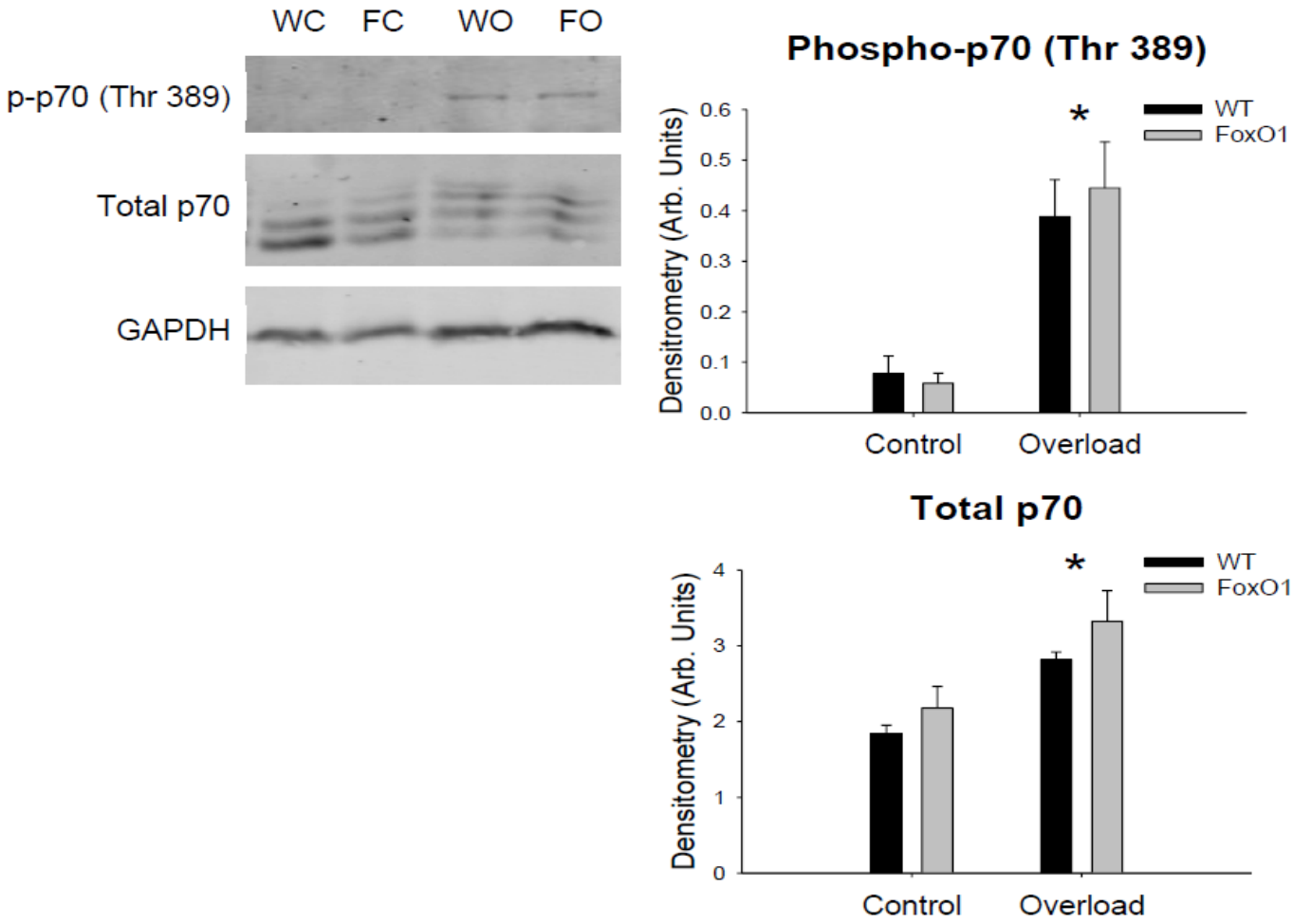

Figure 5. Phosphorylated and Total $p70^{s6k}$ Protein in Control and Overloaded Plantaris Muscles of Wildtype and $FoxO1^{+/-}$ Mice. Panel A: Representative western blot analyses from wildtype control (WC), $FoxO1^{+/-}$ control (FC), wildtype ablation (WO) and $FoxO1^{+/-}$ ablation (FO) conditions. Panels B and C: Quantification of western blot data for phosphorylated and total $p70^{s6k}$, respectively. *, significant main effect for treatment. $P<0.05$ for all significant differences. n=6 for all groups. Data represented as means ± standard error.

Phosphorylated 4EBP-1 had a tendency to be elevated in the muscles of FoxO1$^{+/-}$ mice (P=0.09; Figures 6A and 6B). However, when expressed as a ratio of total:phosphorylated protein, any potential difference was eliminated (Figure 6D). Mechanical overload resulted in significantly decreased total 4EBP-1 protein expression (Figure 6C) and the difference remained significant when expressed as the total:phosphorylated ratio (Figure 6D).

Figure 6

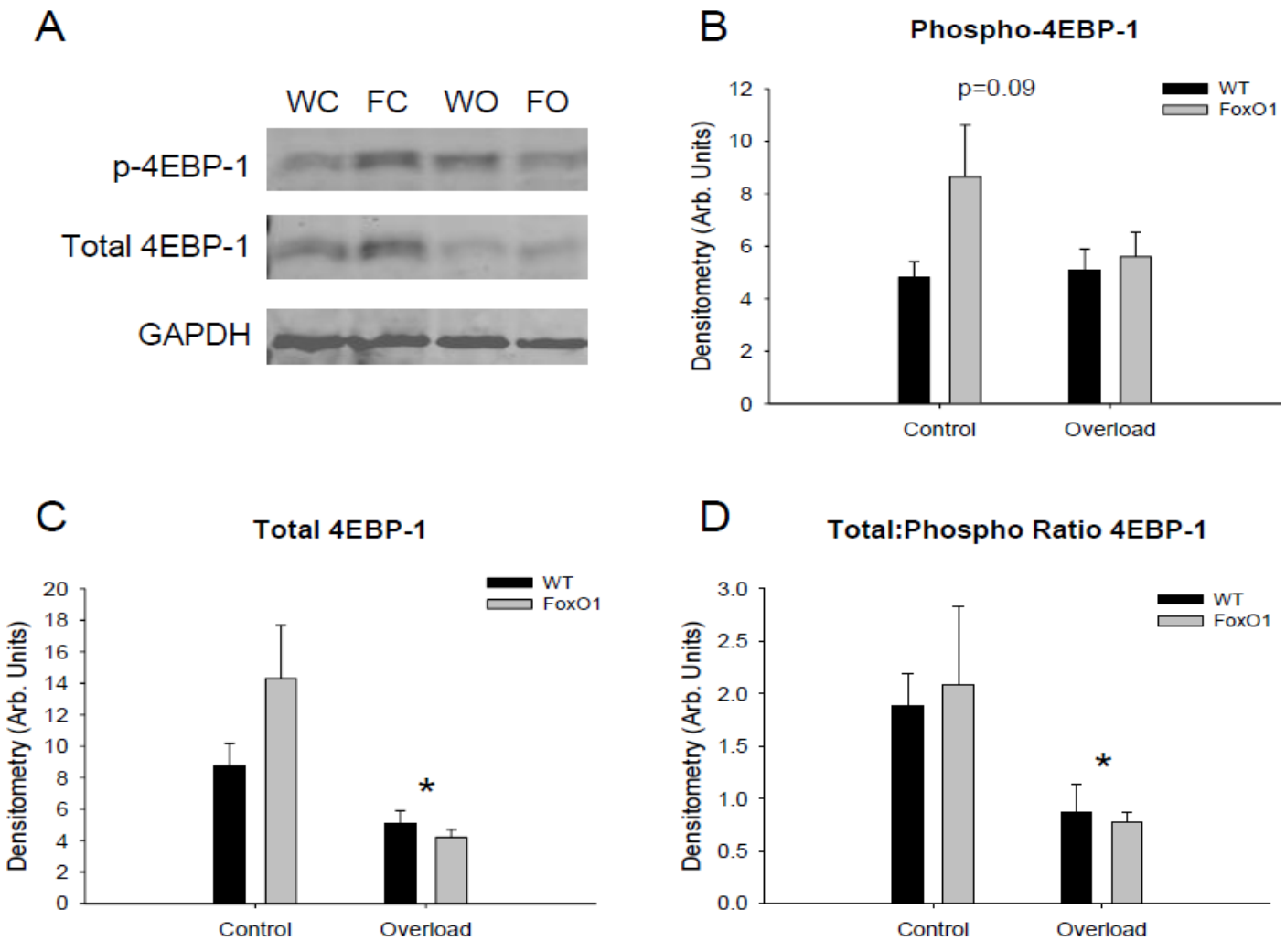

Figure 6. Phosphorylated and Total 4EBP-1 Protein in Control and Overloaded Plantaris Muscles of Wildtype and FoxO1$^{+/-}$ Mice. Panel A: Representative western blot analyses from wildtype control (WC), FoxO1$^{+/-}$ control (FC), wildtype ablation (WO) and FoxO1$^{+/-}$ ablation (FO) conditions. Panels B and C: Quantification of western blot data for phosphorylated and total 4EBP-1, respectively. Panel D: Total:phosphorylated 4EBP-1 ratio. &, trend for significant main effect for strain (P=0.09); *, significant main effect for treatment. P<0.05 for all significant differences. n=6 for all groups. Data represented as means ± standard error.

FoxO1-mediated inhibition of muscle hypertrophy is associated with elevations in MAFbx/atrogin-1 gene and protein expression. MAFbx/atrogin-1 gene expression was globally elevated in FoxO1$^{+/-}$ mice compared to WT mice and mechanical overload resulted in a significant decrease in MAFbx/atrogin-1 gene expression compared to control muscle (Figure 7A). Protein levels of MAFbx/atrogin-1 were not globally different between mouse strains; however, mechanical overload resulted in significant reductions in MAFbx/atrogin-1 protein expression in FoxO1$^{+/-}$ and WT mice compared to their respective controls (Figure 7B and 7C). Further, FoxO1$^{+/-}$ control samples displayed significantly elevated MAFbx/atrogin-1 protein compared to all other groups. Although MAFbx/atrogin-1 gene expression was globally elevated in FoxO1$^{+/-}$, total protein ubiquination was not different between strains and did not appear to change after overload (Figure 7D).

Figure 7

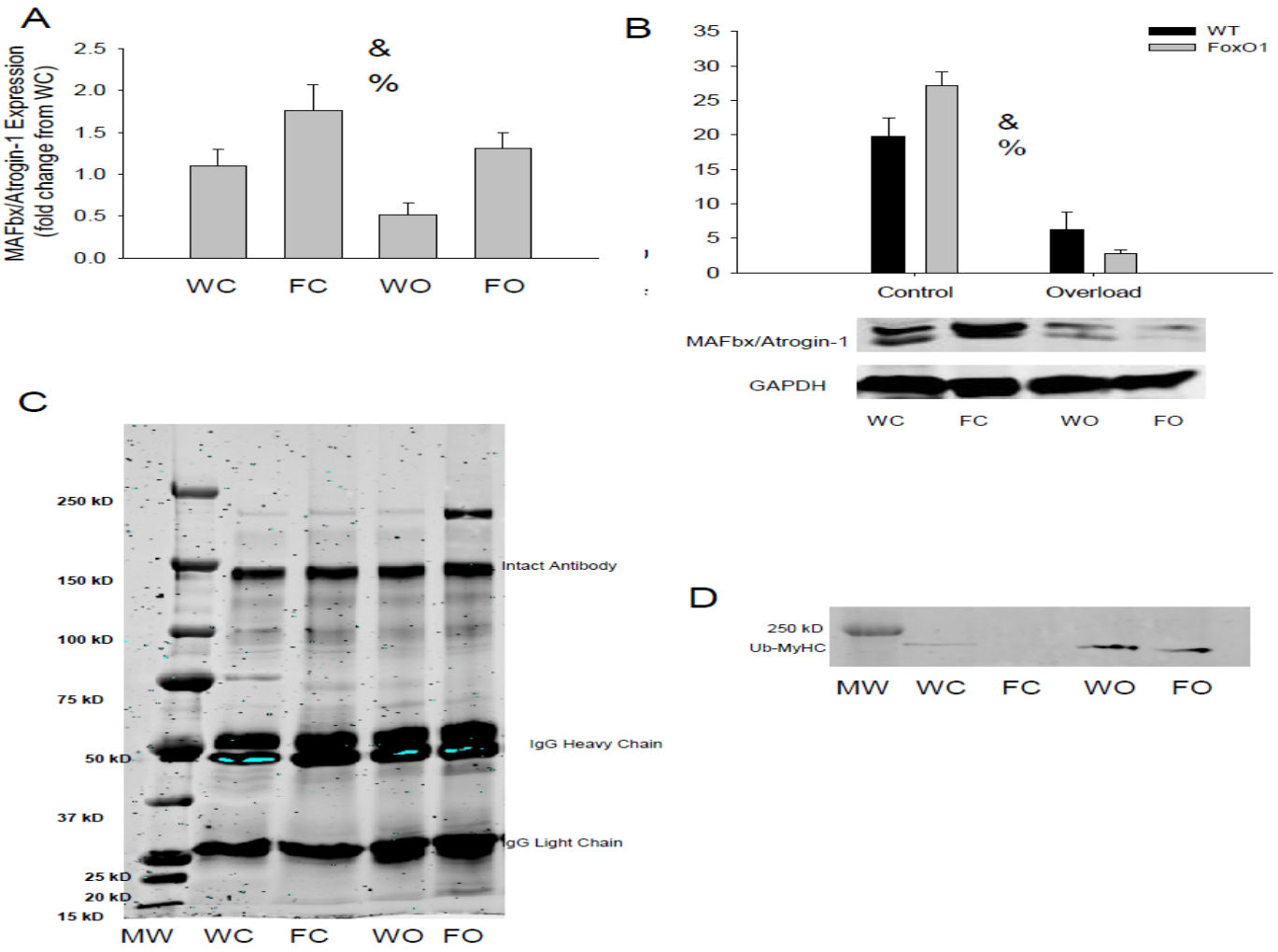

Figure 7. MAFbx/Atrogin-1 Gene Expression and Protein Ubiquination in Control and Overloaded Plantaris Muscles of Wildtype and FoxO1$^{+/-}$ Mice. (A) MAFbx/Atrogin-1 gene expression, (B) Ubiquinated myosin heavy chain, and (C) Krypton stain for total protein ubiquination. Lanes identified as wildtype control (WC), FoxO1$^{+/-}$ control (FC), wildtype ablation (WO) and FoxO1$^{+/-}$ ablation (FO) conditions. &, significant main effect for strain; %, significant main effect for treatment. $P<0.05$ for all significant differences. n=4-6 for all groups. Data represented as means ± standard error.

DISCUSSION

The findings from this study demonstrate that FoxO1 overexpression in skeletal muscle suppresses muscle hypertrophy. Markers of muscle hypertrophy including, total protein content, muscle mass, and muscle fiber cross-sectional area increased following 2 wks of mechanical overload. However, FoxO1 overexpression in skeletal muscle resulted in a dampened response compared to the observed increases in age-matched wildtype animals. Opposite our hypotheses, the above noted differences between mouse strains do not appear to be a result of quelled anabolic signaling through Akt, mTOR or the associated downstream targets as no evident changes in phosphorylation status of these proteins was detected. Additionally, the subdued response in hypertrophy observed with overexpression of FoxO1 does not appear to be caused by an increase in catabolic activity of the E3 ubiquitin ligase MAFbx/Atrogin-1. Although proteolytic machinery was likely enhanced as a result of increased FoxO1 expression, (globally higher MAFbx/atrogin-1 gene and protein expression in FoxO1 overexpressing mice), mechanical overload significantly reduced MAFbx/atrogin-1 gene and protein expression in both mouse strains to a similar degree and there was no effect of FoxO1 overexpression on protein ubiquination. As such, our contention is that the decreased muscle size conferred through FoxO1 overexpression is independent of signaling through the canonical Akt/mTOR pathway.

The balance between protein synthesis and protein degradation pathways in skeletal muscle hypertrophy was recently examined by Stitt et al.(32) in which they showed that activation of Akt was associated with a downregulation of the noted protein ubiquination genes, MuRF-1 and MAFbx/atrogin-1 in cultured muscle cells. Interestingly, the supression in MuRF-1 and MAFbx/atrogin-1 expression appeared to be largely mediated through FoxO1 as introduction of mutant FoxO1 that is not responsive to Akt signaling prevented Akt-mediated suppression of MuRF-1 and MAFbx/atrogin-1 gene activity (32). The link between FoxO transcription factors and muscle size regulation has been further substantiated through in vitro analyses using genetic downregulation models. Specifically, Sandri et al. (31) reported that muscle atrophy induced through serum starvation or glucocorticoid administration was associated with reductions in Akt-mediated signaling and promotion of MAFbx/atrogin-1 gene expression. The increased MAFbx/atrogin-1 gene expression was signficantly blunted via blockade of FoxO activity (FoxO3a; closely related FoxO homologue) through induction of dominant negative forms of FoxO or infusion of inhibitor RNA directed against FoxO. Findings by Kamei et al. (16), using a transgenic mouse model with skeletal muscle specific overexpression of the FoxO1 protein, corrorobrates these in vitro findings by demonstrating that FoxO1 supresses skeletal muscle size and increases the expression of various pro-catabolic genes (e.g., MAFbx/atrogin-1, cathepsin L).

Considering this apparent relationship between FoxO1 and skeletal muscle size and the influence of the Akt and mTOR-mediated signaling on increasing protein synthesis efficiency and/or capacity (9, 17,23,24) and regulation of genes known to boost protein ubiquination and proteosome mediated degradation (16,31,32), our work has focused on investigating the impact of FoxO1 overexpression on the activity of the major components within this complex signaling pathway. Opposite our expectations, overexpression of FoxO1 in skeletal muscle resulted in an enhanced degree of basal level Akt phosphorylation (i.e., non-overloaded muscle) compared to wildtype controls. Interestingly, recent work in multiple cell lines (7) cardiomyocytes (25) has shown that FoxO overexpression results in increases in basal Akt phosphorylation, corroborating our data. Furthermore, Moylan et al. (22) recently reported that Akt phosphorylation was significantly elevated in mouse skeletal muscle cells in vitro in the presence of the known atrophy inducing molecule TNFα. Thus, in keeping with these findings, it appears that muscle atrophy induced through FoxO1 expression occurs not as a result of suppressed Akt activity, but despite enhanced Akt signaling.

Downstream of Akt, mTOR has been shown to be the primary kinase responsible for regulating $p70^{s6k}$ (Thr 389) and 4EBP-1(Thr 37/46) phosphorylation in response to growth stimulus (9,13,23,24). mTOR is found in two protein complexes: TORC1 (mTOR, GßL/LST8, raptor, rheb), which is important for cell growth and TORC2 (mTOR, GßL, rictor), which is involved in cytoskeleton orgranization (33). Recent work by Wu et al. (34) has suggested that overexpression of FoxO1 in myocytes results in suppression of myotube formation. This is due primarily to degradation of certain components of the TORC1 complex and downstream molecular targets, specifically mTOR and $p70^{s6k}$, while other downstream targets, namely Akt and 4EBP-1, remained unchanged (34). Contrary to these findings, our current work suggests that the activity of the purported anabolic mTOR and $p70^{s6k}$ were not attenuated by FoxO1 overexpression when challenged with a growth stimulus. Further, although 4EBP-1 phosphorylation had a tendency to be elevated in the control muscle with FoxO1 overexpression, when expressed as a total: phosphorylation ratio there was no significant effect of FoxO1. Additionally, no overt changes in 4EBP-1 gene expression were found indicating that any potential differences in protein abundance observed were likely the result of post-translational mechanisms.

While $p70^{s6k}$ and 4EBP-1 have received much attention in the realm of regulating skeletal muscle mass there remains controversy as to the significance of their contribution to muscle growth. Although evidence points to the ability of $p70^{s6k}$ to phosphorylate the S6 protein on the 40S ribosomal subunit and subsequently promote protein translation initiation (23,27), cell growth is not always associated with the upregulation of $p70^{s6k}$ as research using genetic manipulations (e.g., $p70^{s6k}$ knockouts) demonstrate cell growth in the absence of $p70^{s6k}$ production (27,33). Furthermore, suggestions that ribosomal S6 acts primarily in the translation of 5' TOP mRNAs upon activation by $p70^{s6k}$ (15) appears controversial, as more recent findings suggest that mutation of S6 phosphorylation sites significantly decreases muscle size but does not impact translation of 5' TOP mRNAs, nor does it suppress protein synthesis (29). In addition, 4E-BP1, an inhibitory binding partner to the eukaryotic initiation factor 4E, has been linked to muscle size regulation as its inactivation has been widely observed in both in vitro and in vivo models of cell growth (1,2,26) and has been linked to the promotion of skeletal muscle protein synthesis (2). Although a role of 4EBP-1 in skeletal muscle size regulation has been shown, as TORC1-mediated phosphorylation of 4E-BP1 results in the subsequent release of eIF4E and formation of the eIF4F-eIF4G complex necessary for translation initiation (2), a clear understanding is still lacking. Additional studies show that blocking the formation of the eIF4F complex does not appear to blunt muscle protein synthesis or mRNA translation (14) and the expression of eIF4E does not rescue muscle cells from atrophy associated with suppression in $p70^{s6k}$ activity (1,26). It is possible that 4E-BP1 regulation of the eIF4F formation may not play a primary role during skeletal muscle hypertrophy.

Our data, taken with the literature, suggests that lack of significant findings in the activity of these signaling molecules associated with Akt and mTOR-mediated signaling may not be surprising given their controversial role in supporting the growth of skeletal muscle. Importantly, the characterized differences in fiber type and running wheel activity of FoxO1 overexpressing mice should be noted. Kamei et al. reported that FoxO1 and associated isoforms (e.g., FoxO3a) have been shown to induce muscle atrophy through induction of genes regulating protein ubiquination and proteasome mediated degradation (16,31,32). As such, we addressed MAFbx/atrogin-1 gene and protein expression and associated protein ubiquination as a potential indicator of protein degradation within skeletal muscle. As reported previously (20), MAFbx/atrogin-1 gene expression was significantly reduced (~50%) following 2-wks of chronic overload, which was consistent with our findings in both the wildtype and FoxO1 overexpressing muscle. In addition, protein levels mirrored the gene expression data as mechanical overload resulted in a reduction of MAFbx/atrogin-1 protein expression compared to control. Thus, despite the significant increase in MAFbx/atrogin-1 gene and protein expression

conferred through FoxO1 expression under basal conditions, the influence of mechanically overloading the muscle resulted in attenuation in MAFbx/atrogin-1 activity.

Moreover, our data has revealed that protein ubiquination appeared unaltered through FoxO1 overexpression. Though muscle mass was lower in control and overloaded muscle of FoxO1 mice, active protein ubiquination does not appear to be the main factor mediating the reduced degree of muscle growth observed. Importantly, previous research has predominantly studied acute muscle atrophy occurring in the hours to days following FoxO1 activation in isolated cell culture environments. Thus, it is possible that in this model of chronic FoxO1 overexpression, degradatory responses may have already culminated resulting in a new set point for muscle mass. Also, it is possible that some mechanisms may be in place within the cell to counteract continued ubiquination and potential degradation of cytoskeletal components conferred through FoxO1 expression. Alternatively, due to the rapid nature in which ubiquinated proteins are degraded by the proteasome, it is possible that FoxO1 overexpression may have amplified the rate of ubiquination and subsequent protein degradation within the muscle that was not captured in the ubiquination assay. Although not significant in control muscle in either mouse strain, MyHC ubiquination was elevated during muscle overload, which occurred concomitantly with an increase in muscle mass and cross sectional area in both mouse strains. This response is not entirely unexpected bearing in mind the rate of protein turnover in exercising muscle and the degree of protein degradation which has been observed in this surgical overload model (10). Further, using a human skeletal muscle hypertrophy model, Leger et al. (19) reported an increased phosphoryation of Akt and mTOR along with nuclear exclusion of FoxO1 in the weeks following resistance training. However, gene expression of MAFbx/atrogin-1 was significantly elevated despite marked increases in muscle cross sectional area (10%). Although the apparent differences between the studies may reflect species variability, differences in hypertrophy induction, and/or time of sampling tissues, it is conceivable that increases in certain pro-catabolic processes may be an integral part in ultimately facilitating skeletal muscle growth. Regardless, FoxO1 overexpression did not appear to differentially regulate MyHC ubiquination during mechanical overload, suggesting that gross loss of contractile elements was not a causative agent of the growth inhibition observed.

CONCLUSION

Overexpression of FoxO1 in skeletal muscle has a strong influence in suppressing skeletal muscle growth. Although the mechanism for this action remains largely elusive, it is unlikely that this suppression in growth is mediated through modulating mTOR and downstream signaling directly. However, further research, specifically experiments focused on the outcome measure of protein synthesis, is necessary to substantiate the ability of FoxO1 to impact anabolism in skeletal muscle. Further research into the mechanisms of action related to FoxO1 in skeletal muscle may provide breakthrough therapies for the treatment of muscle dysfunction associated with diseases of major social impact, such as cardiovascular disease, renal disease, pulmonary disorders, and diabetes.

ACKNOWLEDGMENTS

Supported by a grant through the deArce Memorial Endowment Fund in Support of Medical Research and Development (TJM). The authors wish to thank Zachary Brinkman and Evan Schick for their support with western blot analyses and gene expression assays.

Address for correspondence: Rachael A. Potter, Department of Kinesiology, The University of Toledo, Toledo, Ohio, 43606; Phone: 419-530-2690; Email: Rachael.Hoover@Rockets.utoledo.edu

REFERENCES

1. Anthony JC, Anthony TG, Kimball SR, Vary TC, Jefferson LS. Orally administered leucine stimulates protein synthesis in skeletal muscle of postabsorptive rats in association with increased eIF4F formation. ***J Nutr.*** 2000;130:139-145.

2. Anthony JC, Yoshizawa F, Anthony TG, Vary TC, Jefferson LS, Kimball SR. Leucine stimulates translation initiation in skeletal muscle of postabsorptive rats via a rapamycin-sensitive pathway. ***J Nutr.*** 2000;130:2413-2419.

3. Baar K, Esser K. Phosphorylation of p70(S6k) correlates with increased skeletal muscle mass following resistance exercise. ***Am J Physiol.*** 1999;276:C120-127.

4. Bodine SC, Latres E, Baumhueter S, Lai VK, Nunez L, Clarke BA, Poueymirou WT, Panaro FJ, Na E, Dharmarajan K, Pan ZQ, Valenzuela DM, DeChiara TM, Stitt TN, Yancopoulos GD, Glass DJ. Identification of ubiquitin ligases required for skeletal muscle atrophy. ***Science.*** 2001;294:1704-1708.

5. Bodine SC, Stitt TN, Gonzalez M, Kline WO, Stover GL, Bauerlein R, Zlotchenko E, Scrimgeour A, Lawrence JC, Glass DJ, Yancopoulos GD. Akt/mTOR pathway is a crucial regulator of skeletal muscle hypertrophy and can prevent muscle atrophy in vivo. ***Nat Cell Biol.*** 2001;3:1014-1019.

6. Brunet A, Bonni A, Zigmond MJ, Lin MZ, Juo P, Hu LS, Anderson MJ, Arden KC, Blenis J, Greenberg ME. Akt promotes cell survival by phosphorylating and inhibiting a Forkhead transcription factor. ***Cell.*** 1999;96:857-868.

7. Chen CC, Jeon SM, Bhaskar PT, Nogueira V, Sundararajan D, Tonic I, Park Y, Hay N. FoxOs inhibit mTORC1 and activate Akt by inducing the expression of Sestrin3 and Rictor. ***Dev Cell.*** 2010;18:592-604.

8. Dreyer HC, Glynn EL, Lujan HL, Fry CS, Dicarlo SE, Rasmussen BB. Chronic paraplegia-induced muscle atrophy downregulates the mTOR/S6K1 signaling pathway. ***J Appl Physiol.*** 2008;104(1):27-33.

9. Farrell PA, Hernandez JM, Fedele MJ, Vary TC, Kimball SR, Jefferson LS. Eukaryotic initiation factors and protein synthesis after resistance exercise in rats. ***J Appl Physiol.*** 2000;88:1036-1042.

10. Goldspink DF, Garlick PJ, McNurlan MA. Protein turnover measured in vivo and in vitro in muscles undergoing compensatory growth and subsequent denervation atrophy. ***Biochem J.*** 1983;210:89-98.

11. Gomes MD, Lecker SH, Jagoe RT, Navon A, Goldberg AL. Atrogin-1, a muscle-specific F-box protein highly expressed during muscle atrophy. ***Proc Natl Acad Sci U S A.*** 2001;98: 14440-14445.

12. Hornberger TA, McLoughlin TJ, Leszczynski JK, Armstrong DD, Jameson RR, Bowen PE, Hwang ES, Hou H, Moustafa ME, Carlson BA, Hatfield DL, Diamond AM, Esser KA. Selenoprotein-deficient transgenic mice exhibit enhanced exercise-induced muscle growth. ***J Nutr.*** 2003;133:3091-3097.

13. Hornberger TA, Sukhija KB, Wang XR, Chien S. mTOR is the rapamycin-sensitive kinase that confers mechanically-induced phosphorylation of the hydrophobic motif site Thr(389) in p70(S6k). ***FEBS Lett.*** 2007;581:4562-4566.

14. Huang BP, Wang Y, Wang X, Wang Z, Proud CG. Blocking eukaryotic initiation factor 4F complex formation does not inhibit the mTORC1-dependent activation of protein synthesis in cardiomyocytes. ***Am J Physiol Heart Circ Physiol.*** 2009;296:H505-514.

15. Jefferies HB, Fumagalli S, Dennis PB, Reinhard C, Pearson RB, Thomas G. Rapamycin suppresses 5'TOP mRNA translation through inhibition of p70s6k. ***Embo J.*** 1997;16:3693-3704.

16. Kamei Y, Miura S, Suzuki M, Kai Y, Mizukami J, Taniguchi T, Mochida K, Hata T, Matsuda J, Aburatani H, Nishino I, Ezaki O. Skeletal muscle FOXO1 (FKHR) transgenic mice have less skeletal muscle mass, down-regulated Type I (slow twitch/red muscle) fiber genes, and impaired glycemic control. ***J Biol Chem.*** 2004;279:41114-41123.

17. Kubica N, Kimball SR, Jefferson LS, Farrell PA. Alterations in the expression of mRNAs and proteins that code for species relevant to eIF2B activity after an acute bout of resistance exercise. ***J Appl Physiol.*** 2004;96:679-687.

18. Latres E, Amini AR, Amini AA, Griffiths J, Martin FJ, Wei Y, Lin HC, Yancopoulos GD, Glass DJ. Insulin-like growth factor-1 (IGF-1) inversely regulates atrophy-induced genes via the phosphatidylinositol 3-kinase/Akt/mammalian target of rapamycin (PI3K/Akt/mTOR) pathway. ***J Biol Chem.*** 2005;280:2737-2744.

19. Leger B, Cartoni R, Praz M, Lamon S, Deriaz O, Crettenand A, Gobelet C, Rohmer P, Konzelmann M, Luthi F, Russell AP. Akt signalling through GSK-3beta, mTOR and Foxo1 is involved in human skeletal muscle hypertrophy and atrophy. ***J Physiol.*** 2006;576:923-933.

20. Marino JS, Tausch BJ, Dearth CL, Manacci MV, McLoughlin T, Rakyta SJ, Linsenmayer MP, Pizza FX. {beta}2 integrins contribute to skeletal muscle hypertrophy in mice. ***Am J Physiol Cell Physiol.*** 2008;295:1026-1036.

21. McLoughlin TJ, Smith SM, Delong AD, Wang H, Unterman TG, Esser KA. FoxO1 induces apoptosis in skeletal myotubes in a DNA binding-dependent manner. ***Am J Physiol Cell Physiol.*** 2009;297(3):C548-555.

22. Moylan JS, Smith JD, Chambers MA, McLoughlin TJ, Reid MB. TNF induction of atrogin-1/MAFbx mRNA depends on Foxo4 expression but not AKT-Foxo1/3 signaling. ***Am J Physiol Cell Physiol.*** 2008;295(4):C986-993.

23. Nader GA, Hornberger TA, Esser KA. Translational control: Implications for skeletal muscle hypertrophy. ***Clin Orthop Relat Res.*** 2000;403:S178-187.

24. Nader GA, McLoughlin TJ, Esser KA. mTOR function in skeletal muscle hypertrophy: Increased ribosomal RNA via cell cycle regulators. ***Am J Physiol Cell Physiol.*** 2005;289: C1457-1465.

25. Ni YG, Wang N, Cao DJ, Sachan N, Morris DJ, Gerard RD, Kuro OM, Rothermel BA, Hill JA. FoxO transcription factors activate Akt and attenuate insulin signaling in heart by inhibiting protein phosphatases. ***Proceedings of the National Academy of Sciences of the United States of America.*** 2007;104:20517-20522.

26. Ohanna M, Sobering AK, Lapointe T, Lorenzo L, Praud C, Petroulakis E, Sonenberg N, Kelly PA, Sotiropoulos A, Pende M. Atrophy of S6K1(-/-) skeletal muscle cells reveals distinct mTOR effectors for cell cycle and size control. ***Nat Cell Biol.*** 2005;7:286-294.

27. Pende M, Um SH, Mieulet V, Sticker M, Goss VL, Mestan J, Mueller M, Fumagalli S, Kozma SC, Thomas G. S6K1(-/-)/S6K2(-/-) mice exhibit perinatal lethality and rapamycin-sensitive 5'-terminal oligopyrimidine mRNA translation and reveal a mitogen-activated protein kinase-dependent S6 kinase pathway. ***Mol Cell Biol.*** 2004;24:3112-3124.

28. Rena G, Guo S, Cichy SC, Unterman TG, Cohen P. Phosphorylation of the transcription factor forkhead family member FKHR by protein kinase B. ***J Biol Chem.*** 1999;274:17179-17183.

29. Ruvinsky I, Sharon N, Lerer T, Cohen H, Stolovich-Rain M, Nir T, Dor Y, Zisman P, Meyuhas O. Ribosomal protein S6 phosphorylation is a determinant of cell size and glucose homeostasis. ***Genes Dev.*** 2005;19:2199-2211.

30. Sacheck JM, Hyatt JP, Raffaello A, Jagoe RT, Roy RR, Edgerton VR, Lecker SH, Goldberg AL. Rapid disuse and denervation atrophy involve transcriptional changes similar to those of muscle wasting during systemic diseases. ***FASEB J.*** 2007;21:140-155.

31. Sandri M, Sandri C, Gilbert A, Skurk C, Calabria E, Picard A, Walsh K, Schiaffino S, Lecker SH, Goldberg AL. Foxo transcription factors induce the atrophy-related ubiquitin ligase atrogin-1 and cause skeletal muscle atrophy. ***Cell.*** 2004;117:399-412.

32. Stitt TN, Drujan D, Clarke BA, Panaro F, Timofeyva Y, Kline WO, Gonzalez M, Yancopoulos GD, Glass DJ. The IGF-1/PI3K/Akt pathway prevents expression of muscle atrophy-induced ubiquitin ligases by inhibiting FOXO transcription factors. ***Mol Cell.*** 2004;14:395-403.

33. Wang X, Proud CG. The mTOR pathway in the control of protein synthesis. ***Physiology (Bethesda).*** 2006;21:362-369.

34. Wu AL, Kim JH, Zhang C, Unterman TG, Chen J. Forkhead box protein O1 negatively regulates skeletal myocyte differentiation through degradation of mammalian target of rapamycin pathway components. ***Endocrinology.*** 2008;149:1407-1414.

35. Zhang X, Gan L, Pan H, Guo S, He X, Olson ST, Mesecar A, Adam S, Unterman TG. Phosphorylation of serine 256 suppresses transactivation by FKHR (FOXO1) by multiple mechanisms. Direct and indirect effects on nuclear/cytoplasmic shuttling and DNA binding. ***J Biol Chem.*** 2002;277:45276-45284.